Acta Crystallographica Section F
Structural Biology and Crystallization Communications
ISSN 1744-3091

Purification, crystallization and preliminary X-ray analysis of glutathione peroxidase Gpx3 from *Saccharomyces cerevisiae*

Zhu Yang and Cong-Zhao Zhou*

Hefei National Laboratory for Physical Sciences at Microscale and School of Life Sciences, University of Science and Technology of China, Hefei, Anhui 230027, People's Republic of China

Correspondence e-mail: zcz@ustc.edu.cn

Received 22 March 2006
Accepted 14 May 2006

The glutathione peroxidase Gpx3 from the yeast *Saccharomyces cerevisiae* has been overexpressed, purified and crystallized. Both gel-filtration and dynamic light-scattering (DLS) results indicate that Gpx3 is a monomer in solution at a concentration of about 2 mg ml^{-1}, whereas glutathione peroxidases are normally tetrameric or dimeric. X-ray diffraction data from a single crystal of Gpx3 have been collected to 2.6 Å resolution. The crystals are triclinic and belong to space group $P1$, with unit-cell parameters a = 38.187, b = 43.372, c = 56.870 Å, α = 71.405, β = 73.376, γ = 89.633°. There are two Gpx3 monomers in a crystallographic asymmetric unit. Preliminary analyses show that the yeast Gpx3 is quite different from those of mammals.

1. Introduction

All aerobic organisms are exposed to reactive oxygen species (ROS) such as hydrogen peroxide (H_2O_2), superoxide anion (O_2^-) and hydroxyl radical ($OH^{\cdot}$). Oxidative stress occurs when cellular survival mechanisms are unable to cope with ROS or the damage they cause (Basu *et al.*, 2004; Inoue *et al.*, 1999). Glutathione peroxidase is believed to protect cells against oxidative challenge and catalyzes the reduction of a variety of hydroperoxides with the reaction stoichiometry

$$ROOH + 2GSH \rightarrow ROH + H_2O + GSSG,$$

where GSSG is oxidized glutathione (Epp *et al.*, 1983).

The yeast *Saccharomyces cerevisiae* expresses three glutathione peroxidases (Gpxs) to protect yeast against not only nonphospholipid hydroperoxides but also phospholipid peroxides (Avery & Avery, 2001). In fact, the three genes previously proposed to encode Gpxs encode phospholipid hydroperoxide glutathione peroxidases (PHGPXs). PHGPX is the principal cellular enzyme which is required for membrane lipid peroxidation repair and is the main defence against oxidative membrane damage (Avery & Avery, 2001; Tanaka *et al.*, 2005).

It has recently been reported that Gpx3 also functions as a sensor and transducer of hydroperoxide signal to Yap1, a transcription factor critical for oxidative-stress response in *S. cerevisiae* (Delaunay *et al.*, 2002; Moye-Rowley, 2003; Gulshan *et al.*, 2005). It was concluded that Cys36 of Gpx3, which corresponds to the active SeCys in mammalian Gpx, is oxidized directly to Cys36-SOH by H_2O_2, yielding H_2O (Ellis & Poole, 1997; Claiborne *et al.*, 1999). Cys598 of Yap1, which is located in the C-terminal cysteine-rich domain (c-CRD), reacts with Cys36-SOH to form the Gpx3–Yap1 disulfide linkage. Subsequently, the intermolecular disulfide bridge is attacked by Cys303 of Yap1, which is located in the N-terminal cysteine-rich domain (n-CRD). Consequently, an intramolecular disulfide bond is formed within Yap1 and Gpx3 reverts to the reduced form. Additionally, if Yap1 is absent, Cys82 of Gpx3 attacks the Cys36-SOH to form an intramolecular disulfide bond and this disulfide bond can be reduced by thioredoxins. Thus, Gpx3 functions as a hydroperoxide receptor and redox signal transducer.

For all eukaryotic SeCys-containing glutathione peroxidases characterized to date, it has been found that the selenocysteine

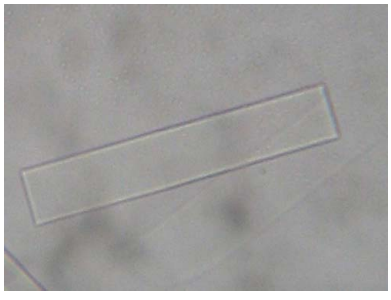

(SeCys) at the active site is encoded by the codon TGA, which is usually a nonsense codon. The cysteine residue of non-selenium-dependent glutathione peroxidases is encoded by codon TGC or TGT (Rocher *et al.*, 1992; Maiorino *et al.*, 2003). Thus, the three yeast Gpxs are non-selenium-dependent glutathione peroxidases as deduced from their coding sequences.

The conversion of SeCys to Cys in mammalian Gpx reduces the enzyme activity drastically (Rocher *et al.*, 1992) and PHGPXs with a Cys at the active site generally have lower activity than those with a SeCys (Delaunay *et al.*, 2002; Hazebrouck *et al.*, 2000). Therefore, the catalytic mechanism of the non-SeCys PHGPX homologues including yeast Gpx1–3 is of considerable interest and the structure of Gpx3 will be helpful to clarify the catalytic mechanism.

2. Materials and methods

2.1. Cloning, expression and purification

The coding region for the GPX3 gene was amplified by PCR with *S. cerevisiae* S288C genomic DNA as the template and inserted into a modified pET28a vector between the *Nde*I and *Not*I sites, with an additional six-His coding sequence at the 5′-end of the genes. The construct was transformed into *Escherichia coli* Rosetta (DE3) (Novagen) and the transformant bacteria were grown in 2×YT medium at 310 K to an $A_{600\,\mathrm{nm}}$ of 1.0. Expression of Gpx3 was induced by adding 0.2 m*M* IPTG (BBI) and the cells were grown for a

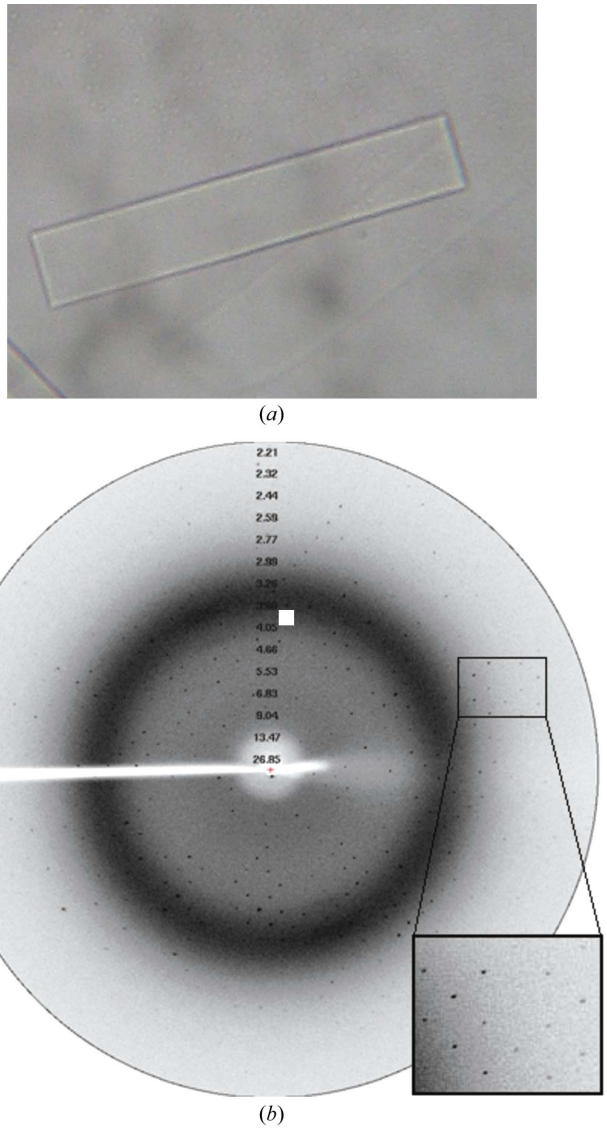

Figure 1
(*a*) Diffraction-quality crystal of Gpx3. (*b*) X-ray diffraction pattern.

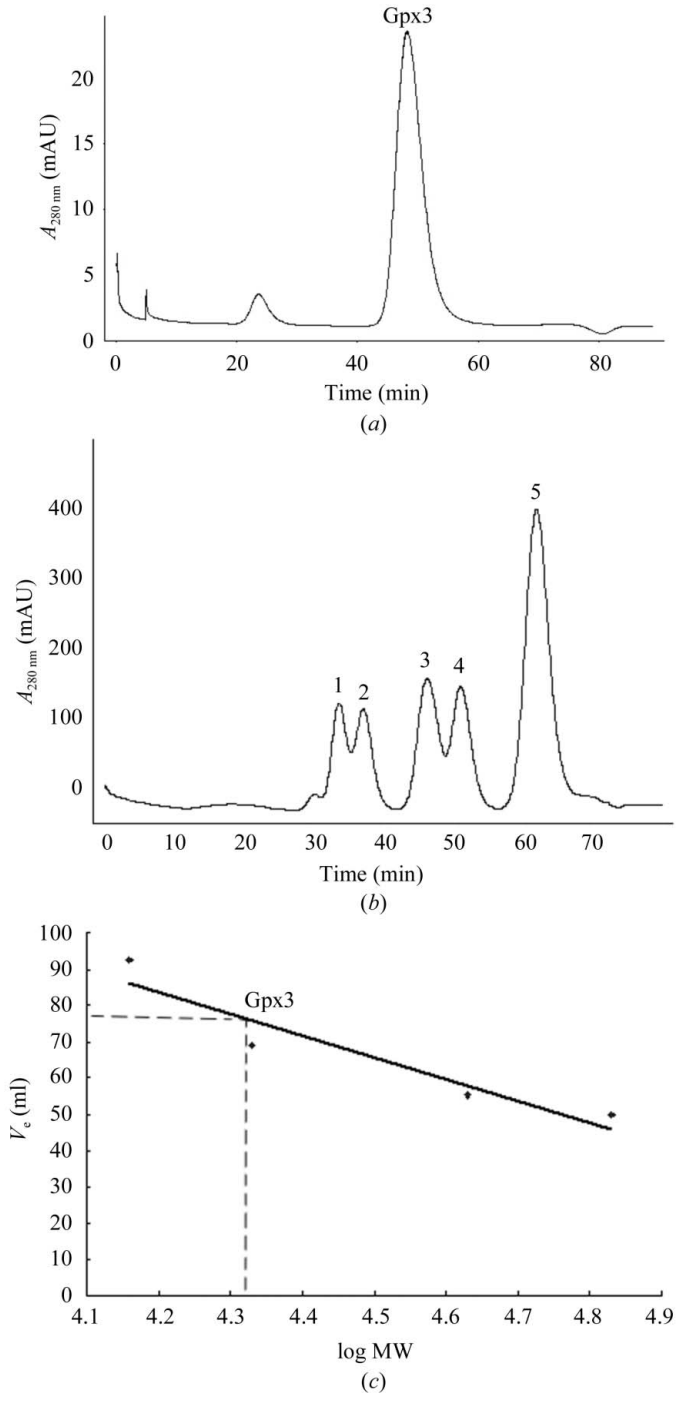

Figure 2
(*a*) Results of gel filtration of Gpx3. The flow rate was 1.5 ml min^{-1}. (*b*) The results of gel filtration of Gpx3 and standard proteins. The flow rate was 1.5 ml min^{-1} and the proteins in the fractions were monitored at 280 nm. Peak 1, albumin, 2 mg ml^{-1}. MW 67 kDa; peak 2, ovalbumin, 2 mg ml^{-1}, MW 43 kDa; peak 3, dual-specificity protein phosphatase VHR, 1 mg ml^{-1}, 21.2 kDa; peak 4, Gpx3, 1 mg ml^{-1}; peak 5, lysozyme, 4 mg ml^{-1}, MW 14.4 kDa. (*c*) The standard curve for molecular weight. V_e of Gpx3 is 77 ml.

Table 1
Data-collection statistics for crystals of Gpx3.

Values in parentheses are for the last resolution shell.

Space group	*P*1
Wavelength (Å)	1.54179
Unit-cell parameters (Å, °)	a = 38.187, b = 43.372, c = 56.870, α = 71.405, β = 73.376, γ = 89.633
Resolution (Å)	2.6
Total No. of reflections	19301
No. of unique reflections	9307
No. of molecules per ASU	2
Completeness (%)	92.1 (88.8)
$R_{\rm merge}$† (%)	14.01 (20.64)

† $R_{\rm merge} = \sum |I_i - \langle I_i \rangle| / \sum \langle I_i \rangle$, where I_i is the observed intensity and $\langle I_i \rangle$ is the average intensity over symmetry-equivalent reflections.

further 16 h. Cells were collected by centrifugation. The pellets were resuspended in 30 ml 20 m*M* Tris–HCl pH 7.0, 200 m*M* NaCl and 14 m*M* β-mercaptoethanol. After being lysed by three cycles of freeze–thawing followed by sonication, the soluble proteins in the supernatant were recovered by centrifugation at 20 000*g* for 45 min. The His-tagged proteins were purified using an Ni^{2+}–NTA affinity chromatography column (Amersham Biosciences) followed by gel filtration (HiLoad 16/60 Superdex 75 prep grade, Amersham Biosciences).

2.2. Dynamic light-scattering measurements

Dynamic light-scattering (DLS) experiments were performed at a wavelength of 824.3 nm using a fixed scattering angle (90°) DynaPro MS800 DLS instrument with a temperature-controlled microsampler at 298 K. The samples were centrifuged at 14 000*g* for 15 min to remove air bubbles and subsequently injected into a 12 µl quartz cuvette. The protein concentration was about 2 mg ml^{-1} in 20 m*M* Tris–HCl pH 7.0 and 200 m*M* NaCl. Data were collected and analyzed using *DYNAMICS* v.6. The molecular weight of the protein was calculated from the hydrodynamic radius.

2.3. Crystallization and preliminary X-ray analysis

Gpx3 was crystallized using the hanging-drop vapour-diffusion method at 289 K. The crystals were grown from a mixture of equal volumes of 3.5 mg ml^{-1} protein in 20 m*M* Tris–HCl pH 7.0, 14 m*M* β-mercaptoethanol, 20 m*M* NaCl and a 400 µl reservoir solution consisting of 25–30% PEG 3350, 0.1 *M* sodium acetate pH 4.8 and 0.02 *M* magnesium chloride (Fig. 1*a*). The crystals crystals grew with a rectangular profile to dimensions of 0.05–0.1 mm within 4 d and diffraction data were collected with an in-house X-ray generator (Rigaku Corporation) and a MAR Research image plate (Fig. 1*b*). For data collection, crystals were flash-frozen after being transferred to crystallization solution containing 30% glycerol

3. Results and discussion

3.1. Gpx3 is monomeric in solution

In contrast to classical glutathione peroxidases, which are normally tetrameric and soluble, PHGPXs are monomeric and partly membrane-associated (Ursini *et al.*, 1995). To check the oligomerization status of Gpx3 in solution, we performed both gel filtration and DLS. As shown in Fig. 2(*a*), Gpx3 is eluted from the HiLoad 16/60 Superdex 75 prep-grade column (Amersham Biosciences) at 77 ml. As shown in Fig. 2, the column was calibrated with standard proteins and the molecular weight of Gpx3 was estimated to be 21 kDa. Fig. 3 shows that the polydispersity (Pd), which refers to the level of homogeneity of the sizes of the particles, is only 13%; particles can be considered to be virtually identical in size or monodisperse when the Pd is less than 15%. The results of DLS show that the radius of Gpx3 is 2.1 nm, corresponding to a molecular weight of 19 kDa. Taken together and compared with the theoretical molecular weight of Gpx3 with a six-His tag (19 500 Da), we conclude that Gpx3 is a monomer in solution at a concentration of about 2 mg ml^{-1} (∼0.2 m*M*) during both experiments.

3.2. Diffraction data of Gpx3 crystal and preliminary crystallographic analyses

The cystal of Gpx3 belongs to the triclinic space group *P*1, with unit-cell parameters a = 38.187, b = 43.372, c = 56.870 Å, α = 71.405, β = 73.376, γ = 89.633°. The data-collection statistics of the best sets are listed in Table 1.

The number of molecules in the asymmetric unit (ASU) was estimated by calculation of the Matthew coefficient and self-rotation function with *MOLREP* (Vagin & Teplyakov, 1997) from the *CCP*4 program package. With the selenocysteine to glycine mutant of human glutathione peroxidase 1 as the search model (PDB code 2f8a), structure solution was found by molecular replacement with *MOLREP*. The rotation angles and the translations were (θ_1 = 125.53, θ_2 = 104.71, θ_3 = 153.08°, t_x = 0, t_y = 0, t_z = 0) and (θ_1 = 241.28, θ_2 = 75.83, θ_3 = 97.64°, t_x = 0.232, t_y = 0.680, t_z = 0.579 Å) for the two molecules, respectively. Further refinement of the structure is in progress.

3.3. Comparison between yeast Gpx1–3 and mammalian Gpx homologues

An alignment of Gpx1–3 with bovine Gpx (PDB code 1gp1) and the selenocysteine to glycine mutant of human Gpx1 (PDB code 2f8a), which are both classic glutathione peroxidases, is shown in Fig. 4. Clearly, the similarity between the mammalian Gpx species is fairly high and the three copies of Gpx in yeast are very highly homologous. However, the yeast Gpx sequences are very different from their mammalian counterparts. It is worth mentioning that a large part of the bovine Gpx sequence (positions 125–142) is deleted in the yeast Gpxs. The missing part in the yeast Gpx paralogues results in a large gap when they are aligned with the sequences of 1gp1 and 2f8a. This part corresponds precisely to the subunit-interaction sites of the tetrameric bovine Gpx (Epp *et al.*, 1983). This

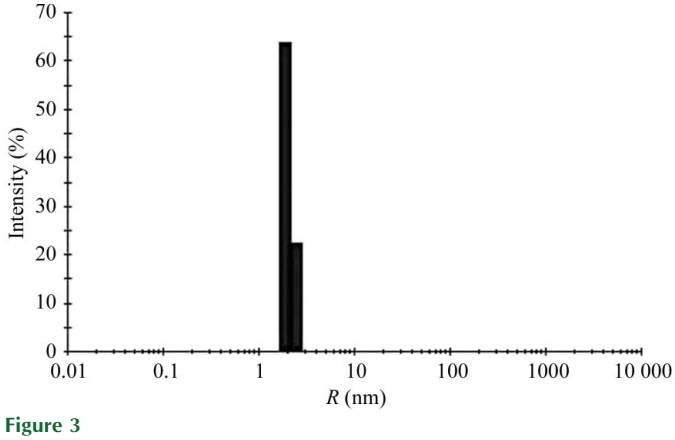

Figure 3
The monomodal size-distribution histogram of Gpx3. x axis of histogram, discrete particle sizes; y axis, percentage intensity (relative amount of light scattered by each bin). The histogram has one peak (a monomodal size distribution). The peak is defined by the mean value (2.1 nm) and polydispersity (13.0%).

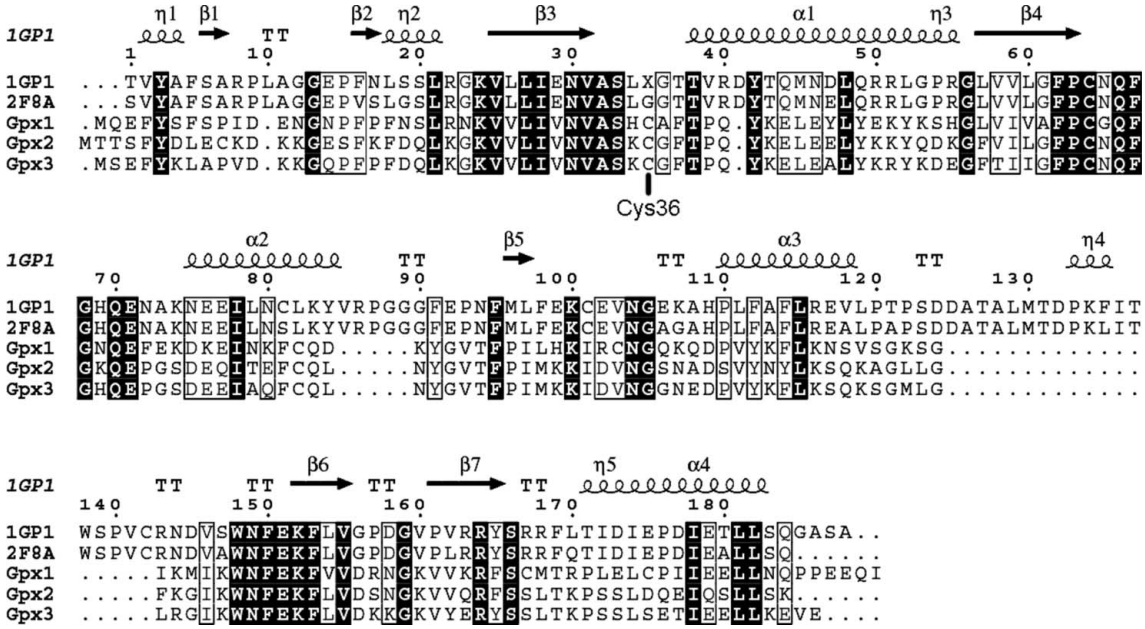

Figure 4
Alignment of yeast Gpxs (Gpx1, Gpx2 and Gpx3) with bovine Gpx (PDB code 1gp1) and the selenocysteine to glycine mutant of human Gpx1 (PDB code 2f8a). The position numbering of the 1gp1 sequence is used throughout. Residues conserved in the three types of Gpx are shaded. The secondary structure of 1gp1 is shown on the top line. The Cys36 which is the active site of Gpx3 is labelled and the X in 1gp1 represents SeCys.

gap was also found in the pig PHGPX sequence (Brigelius-Flohe *et al.*, 1994). It seems likely that the monomeric nature of the phospholipid glutathione peroxidase Gpx3 is critical to facilitate its interaction with the target proteins (*e.g.* Yap1) and its capacity for membrane association. Hopefully, the refined structure of Gpx3 will offer an opportunity for comprehensive understanding of its structure-based molecular function.

We thank Ya-Jun Tang for her assistance during cloning and Zhi-Qiang Zhu for his support during data collection and processing. This work was funded by the Chinese National Natural Science Foundation (grant No. 30470366), the Hundred Talents Project of the Chinese Academy of Science and a Start-up Fund from the University of Science and Technology of China (USTC).

References

Avery, A. M. & Avery, S. V. (2001). *J. Biol. Chem.* **276**, 33730–33735.
Basu, U., Southron, J. L., Stephens, J. L. & Taylor, G. J. (2004). *Mol. Genet. Genomics*, **271**, 627–637.
Brigelius-Flohe, R., Aumann, K. D., Blocker, H., Gross, G., Kiess, M., Kloppel, K. D., Maiorino, M., Roveri, A., Schuckelt, R., Ursini, F., Wingender, E. & Flohe, L. (1994). *J. Biol. Chem.* **269**, 7342–7348.
Claiborne, A., Yeh, J. I., Mallett, T. C., Luba, J., Crane, E. J., Charrier, V. & Parsonage, D. (1999). *Biochemistry*, **38**, 15407–15416.
Delaunay, A., Pflieger, D., Barrault, M. B., Vinh, J. & Toledano, M. B. (2002). *Cell*, **111**, 471–481.
Ellis, H. R. & Poole, L. B. (1997). *Biochemistry*, **36**, 13349–13356.
Epp, O., Ladenstein, R. & Wendel, A. (1983). *Eur. J. Biochem.* **133**, 51–69.
Gulshan, K., Rovinsky, S. A., Coleman, S. T. & Moye-Rowley, W. S. (2005). *J. Biol. Chem.* **280**, 40524–40533.
Hazebrouck, S., Camoin, L., Faltin, Z., Strosberg, A. D. & Eshdat, Y. (2000). *J. Biol. Chem.* **275**, 28715–28721.
Inoue, Y., Matsuda, T., Sugiyama, K. I., Izawa, S. & Kimura, A. (1999). *J. Biol. Chem.* **274**, 27002–27009.
Maiorino, M., Scapin, M., Ursini, F., Biasolo, M., Bosello, V. & Flohe, L. (2003). *J. Biol. Chem.* **278**, 34286–34290.
Moye-Rowley, W. S. (2003). *Eukaryot. Cell*, **2**, 381–389.
Rocher, C., Lalanne, J. L. & Chaudiere, J. (1992). *Eur. J. Biochem.* **205**, 955–960.
Tanaka, T., Lzawa, S. & Inoue, Y. (2005). *J. Biol. Chem.* **280**, 42078–42087.
Ursini, F., Maiorino, M., Brigelius-Flohe, R., Aumann, K. D., Roveri, A., Schomburg, D. & Flohe, L. (1995). *Methods Enzymol.* **252**, 38–53.
Vagin, A. & Teplyakov, A. (1997). *J. Appl. Cryst.* **30**, 1022–1025.